Sign-Error Based Adaptive Control Technique for Single Stage Grid tied SPV System

Shashwat Shivam, Ikhlaq Hussain, *Member, IEEE,* Arpit Jain and Bhim Singh, *Fellow, IEEE*
Dept. of Electrical Engineering, IIT Delhi-110016, India
shashwat.695@gmail.com, ikhlaqb@gmail.com, arpit2602@gmail.com and bhimsinghiitd60@gmail.com

***Abstract*— This paper proposes the use of a sign-error based adaptive control for a three phase single stage grid-tied SPV (Solar Photovoltaic) system. The SPV grid tied system, consists of a SPV array, a voltage source converter (VSC), a ripple filter and three phase loads (balanced and unbalanced) connected to a 3 phase AC grid. The SPV array coupled with the VSC does two tasks namely: 1) provides active power to grid; 2) acts as a distributed static compensator (DSTATCOM). DSTATCOM reduces harmonics in grid current within an IEEE-519 standard, improves power factor and regulates the voltage at the point of common coupling. To maximize the power extracted from the SPV array, the perturb and observe approach is used for maximum power point tracking. The proposed SPV grid tied system is modeled in MATLAB software and its performance is simulated at different loads and changing insolation levels.**

***Index Terms*— Sign-Error, Adaptive Control, SPV, MPPT and Power Quality**

I. Introduction

With the advent of 21st century, it has come a myriad of problems, hitherto underestimated. Global warming, an imminent energy crisis due to unsustainable use of non-renewable sources and climate change have taken the proportions of global crises. However, the increasing use of solar energy is being hailed as a panacea for all the problems which plague humanity today. The solar energy is virtually inexhaustible, pollution and noise free and versatile, thus is perfect to meet the growing demands of energy.

There are two primary ways to interface solar photovoltaic (SPV) arrays with the load which are: 1) standalone mode and 2) grid-integrated mode. The use of an integrated SPV system to grid eliminates the need for a battery or storage unit [1].

The solar power incident at any point on the earth is not constant and is influenced by several parameters such as time of the day, season, atmospheric conditions etc. Thus, a fixed point of operation is not ideal to extract the maximum possible power from the solar energy. To make sure the optimum utilization of solar energy, several maximum power point tracking (MPPT) techniques have been stated in the literature [2]. These techniques operate the SPV array at that voltage where the power extracted from the SPV energy is maximum. Moreover, to increase the efficiency of the system, a single stage topology is used as it has a higher efficiency than a double stage system by order of 2.5% [3].

Primitive SPV systems have been the beset with several problems. The sole purpose fulfilled by the aforementioned systems has been the supply of active power to AC grid and connected loads. The system has a poor power factor and does not eliminate the harmonics introduced into the grid, either due to a nonlinear or unbalanced loads. Recent advances in control algorithms has led to the development of LMF (Least Mean Fourth) [4], adaptive neuro-fuzzy inference system [5], round adaptive detection [6] etc., which perform the functions of a DSTATCOM (Distributed Static Compensator) as well. Moreover, various control algorithms, such as complex wavelet transform [7], combined LMS (Least Mean Square)-LMF [8], ANN (Artificial Neural Network) [9] etc. have been reported in the literature to control the DSTATCOM. Consequently, the grid current would have a low THD (Total Harmonic Distortion) and a power factor close to unity. Moreover, if the load becomes unbalanced, the compensator maintains three phase balanced supply currents in the grid.

In this paper, a sign-error based adaptive control technique for SPV grid-tied system along with the technique of perturb and observe is used to track the MPP (Maximum Power Point). The existing techniques require blocks like PLL, abc to dq converter etc. which increase computational complexity. The proposed sign-error based adaptive algorithm [10] is superior to the conventional algorithms such as SRF (Synchronous Reference Frame) etc; as the computations required are very basic (arithmetic operations) and consequently faster, thereby improving the response of the system. The validity of the concept of proposed control algorithm is verified through simulations in MATLAB software under various conditions like steady state operation, load unbalance and change in irradiance levels.

II. Proposed System Structure And Control Scheme

The proposed SPV grid tied system structure is shown in Fig 1. It comprises of SPV array, a diode, DC link capacitor,

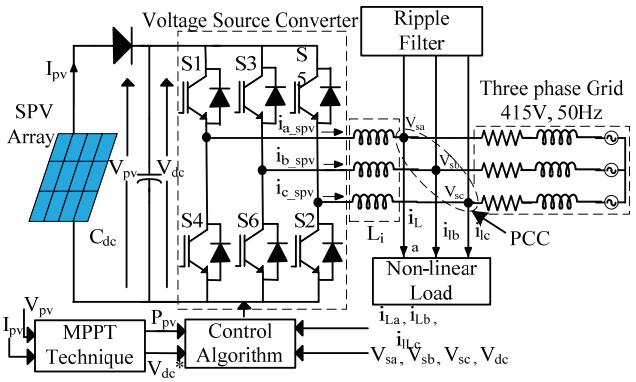

Fig. 1 Proposed system topology

VSC, interfacing inductors (L_i), ripple filters and a three-phase grid with connected linear or nonlinear loads. The capacitor is used to reduce voltage ripples and to stabilize the voltage across the DC bus of the VSC. The VSC consists of IGBT (Insulated Gate Bipolar Transistor) based switches which are controlled through gate signals generated by a sign-error based adaptive control algorithm. It reduces the harmonics and makes the grid voltage nearly sinusoidal. The interfacing inductors are present to eliminate switching ripples in the compensator current while the ripple filter smoothens the grid voltage. The design of the parameters has been reported in the literature [11-12].

Fig. 2 shows the control approach which comprises of the MPPT control and the sign-error control for the switching of VSC. The MPPT control provides a reference DC link voltage and ensures that the point of operation of the system is optimal for extraction of maximum active power from the SPV array. It also calculates the maximum extracted power, P_{pv}, for the calculation of the feed forward term.

The sign-error based control technique is used to extract the fundamental component of load currents and their weight, evaluates the unit template and magnitude of terminal voltage, creates reference grid current and gating signals.

A) Evaluating Amplitude of Terminal Voltage and Unit Templates

Using the phase voltages, (v_{sa}, v_{sb}, v_{sc}) the amplitude of terminal voltage V_t is evaluated as,

$$V_t = \sqrt{\frac{2}{3}\left(v_{sa}^2 + v_{sb}^2 + v_{sc}^2\right)} \quad (1)$$

Using the above, the in-phase unit templates are estimated as,

$$u_{Aa} = \frac{v_{sa}}{V_t}; u_{Ab} = \frac{v_{sb}}{V_t}; u_{Ac} = \frac{v_{sc}}{V_t} \quad (2)$$

The quadrature-phase unit templates can be calculated using the in-phase unit templates as,

$$u_{Ra} = -\frac{u_{Ab}}{\sqrt{3}} + \frac{u_{Ac}}{\sqrt{3}}; u_{Rb} = \frac{\sqrt{3}u_{Aa}}{2} + \frac{u_{Ab} - u_{Ac}}{2\sqrt{3}};$$
$$u_{Rc} = -\frac{\sqrt{3}u_{Aa}}{2} + \frac{u_{Ab} - u_{Ac}}{2\sqrt{3}} \quad (3)$$

B) Calculating Active and Reactive Loss Components

The voltage error, $V_{te}(n)$, is defined as the difference between the voltage of PCC (Point of Common Coupling) and reference value of terminal voltage(V_{tn}), is passed through an AC voltage PI (Proportional Integral) controller. The k^{th} sampled error and the reactive loss component termed w_{cR} are expressed as,

$$V_{te}(k) = V_{tn}(k) - V_t(k) \quad (4)$$

$$w_{cR}(k+1) = w_{cR}(k) + K_{pR}\left(V_{te}(k+1) - V_{te}(k)\right) + K_{iR} \cdot V_{te}(k+1) \quad (5)$$

Here K_{pR} and K_{iR} are the coefficients of the PI controller used. In a similar fashion, the DC voltage error can be calculated as,

$$V_{dce}(k) = V_{dc}^*(k) - V_{dc}(k) \quad (6)$$

Where V_{dc}*(k) is the reference DC link voltage generated from MPPT control.

This is fed through another PI controller for the calculation of the active loss component, w_{cA}, which regulates the DC link voltage.

$$w_{cA}(k+1) = w_{cA}(k) + K_{pA}(V_{dce}(k+1) - V_{dce}(k)) + K_{iA} \cdot V_{dce}(k+1) \quad (7)$$

Here K_{pA} and K_{iA} are the coefficients of the DC bus voltage controller used.

The feed-forward term of solar PV contribution is estimated as,

$$w_{pv}(k) = \frac{2P_{pv}(k)}{3V_t} \quad (8)$$

Here P_{pv} is the extracted SPV power.

C)Extraction of Weights of Load Current

The fundamental active weight component of phase 'a' is calculated as:

$$w_{Aa}(k+1) = w_{Aa}(k) + \tau_A \times u_{Aa}(k) \times \mathrm{sgn}(e_{Aa}(k)) \quad (9)$$

The factor τ_A is set such that good convergence is obtained.

$$e_{Aa}(k) = i_{La}(k) - u_{Aa}(k) \times w_{Aa}(k) \quad (10)$$

Where $e_{Aa}(k)$, $i_{La}(k)$, $u_{Aa}(k)$ and $w_{Aa}(k)$ are the error of the adaptive component, load current, in-phase unit template and weight of active reference component at the k^{th} instant respectively for phase a.

Likely, the weights of fundamental active components of the other phases are calculated as,

$$w_{Ab}(k+1) = w_{Ab}(k) + \tau_A \times u_{Ab}(k) \times \mathrm{sgn}(e_{Ab}(k)) \quad (11)$$

$$w_{Ac}(k+1) = w_{Ac}(k) + \tau_A \times u_{Ac}(k) \times \mathrm{sgn}(e_{Ac}(k)) \quad (12)$$

For calculation of weight of fundamental reactive component of phase 'a', a term $w_{Ra}(k+1)$ is estimated as,

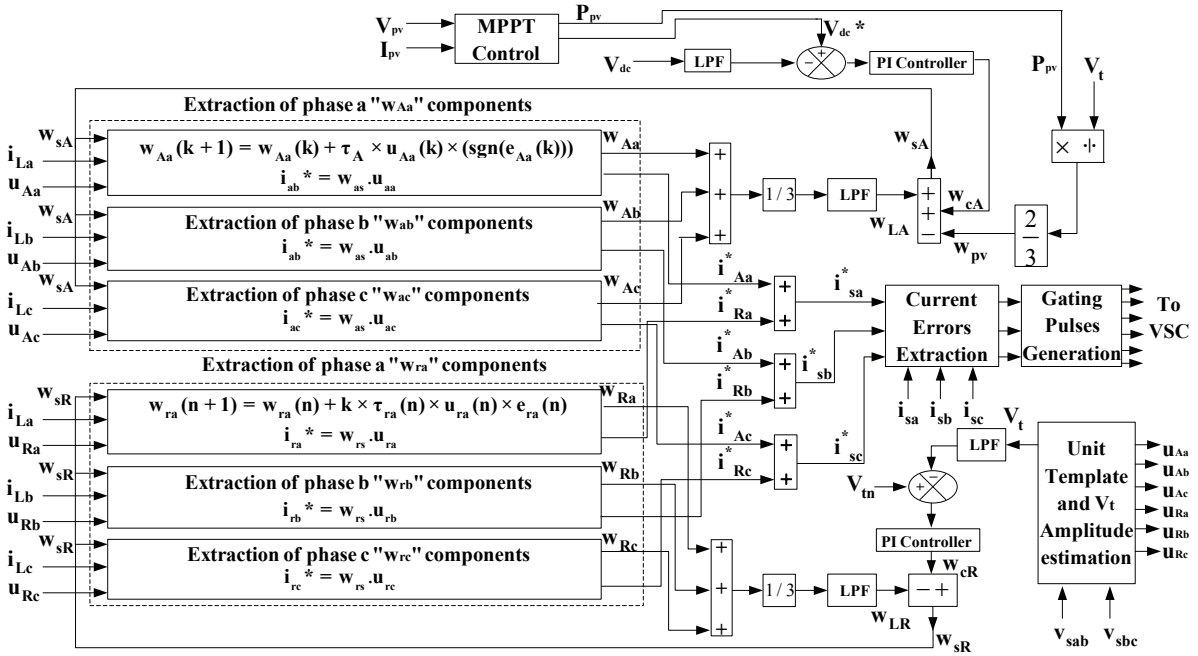

Fig. 2 Structure of sign-error based control algorithm with MPPT control

$$w_{Ra}(k+1) = w_{Ra}(k) + \tau_R \times u_{Ra}(k) \times \text{sgn}(e_{Ra}) \quad (13)$$

The factor τ_R is set such that good convergence is obtained.

$$e_{Ra}(k) = i_{La}(k) - u_{Ra}(k) \times w_{Ra}(k) \quad (14)$$

Where $e_{Ra}(k)$, $i_{La}(k)$, $u_{Ra}(k)$ and $w_{Ra}(k)$ are the error of the adaptive component, load current, quadrature-phase unit template and weight of reactive reference component at the k^{th} instant respectively.

Likewise, the weights of fundamental reactive components of the other phases can be calculated as,

$$w_{Rb}(k+1) = w_{Rb}(k) + \tau_R \times u_{Rb}(k) \times \text{sgn}(e_{Rb}) \quad (15)$$

$$w_{Rc}(k+1) = w_{Rc}(k) + \tau_R \times u_{Rc}(k) \times \text{sgn}(e_{Rc}) \quad (16)$$

D) Generation of Reference Three-Phase Grid Currents and Gating Signals

The net active weight component, w_{sA} is calculated by subtracting the feed forward SPV weight from the sum of the average of the fundamental active weight components and the DC loss component.

$$w_{sA} = w_{cA} + w_{LA} - w_{pv} \quad (17)$$

Here, $w_{LA} = (w_{Aa} + w_{Ab} + w_{Ac})/3$

The active component of reference currents are evaluated as,

$$i^*_{Aa} = w_{sA} \cdot u_{Aa};\ i^*_{Ab} = w_{sA} \cdot u_{Ab};\ i^*_{Ac} = w_{sA} \cdot u_{Ac} \quad (18)$$

Likely, the total reactive weight component, w_{sR} is calculated as,

$$w_{sR} = w_{cR} - w_{LR} \quad (19)$$

Where $w_{LR} = (w_{Ra} + w_{Rb} + w_{Rc})/3$

The reference currents of reactive component are calculated as,

$$i^*_{Ra} = w_{sR} \cdot u_{Ra};\ i^*_{Ab} = w_{sR} \cdot u_{Rb};\ i^*_{Rc} = w_{sR} \cdot u_{Rc} \quad (20)$$

Thus, the net grid currents are estimated as,

$$i^*_{sa} = i^*_{Aa} + i^*_{Ra};\quad i^*_{sb} = i^*_{Ab} + i^*_{Rb};\quad i^*_{sc} = i^*_{Ac} + i^*_{Rc} \quad (21)$$

The error signal is calculated as the difference between the reference and sensed grid currents (i_{sa}*, i_{sb}*, i_{sc}* and i_{sa}, i_{sb}, i_{sc} respectively). This signal is then passed through a hysteresis controller with width δ=0.001 for generating gating pulses.

III. RESULTS AND DISCUSSION

The behavior of the grid interfaced SPV system is observed by implementing the model in MATLAB under different operating conditions. The system has been tested for steady state response, response under unbalanced load conditions and under variable insolation levels.

A) Steady State Behavior of Proposed SPV Grid-Tied System

Figs. 3 (a-b) show the steady state response of the proposed sign error based control algorithm for integrating SPV array into the grid. In these figures, the SPV array DC current (I_{pv}), SPV array DC voltage (V_{pv}), SPV array DC power (P_{pv}), VSC-DC link voltage (V_{dc}), active supply power (P_s), reactive supply power (Q_s), three phase grid voltages (v_{sabc}), three phase grid currents (i_{sabc}), load current of phase 'c' (i_{Lc}), reference three phase grid currents (i_s*) and VSC three phase currents (i_{spv}) are shown. Despite the load being nonlinear, it is observed the grid current is mostly devoid of harmonics with a

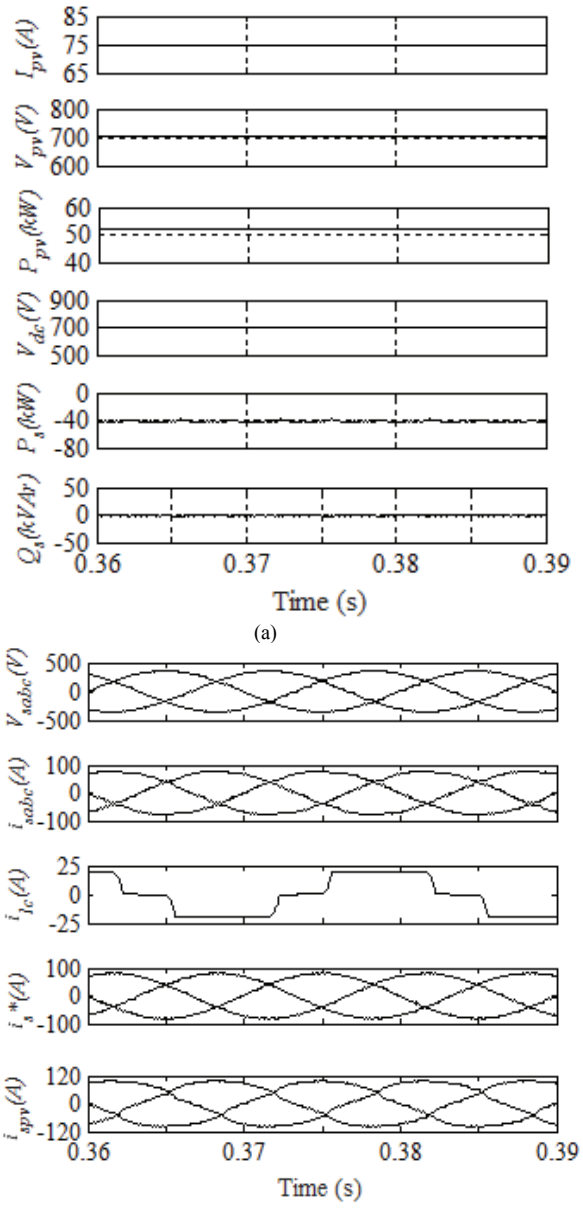

Fig. 3 (a-b) The steady state response of the proposed SPV system

THD of less than 5%, which is under the limit of IEEE-519 standard [13]. Further, the power factor is close to unity, demonstrating that the solar array is delivering power to AC grid. Lastly, the DC link voltage stays constant and nearly 700V.

In Figs. 4 (a-b), the THD of the grid current is 3.19 % which is also within the IEEE-519 standard [13] and the load current has a high THD of 26.55% due to nonlinear nature. The VSC compensates harmonics leading to a reduction in THD of supply current.

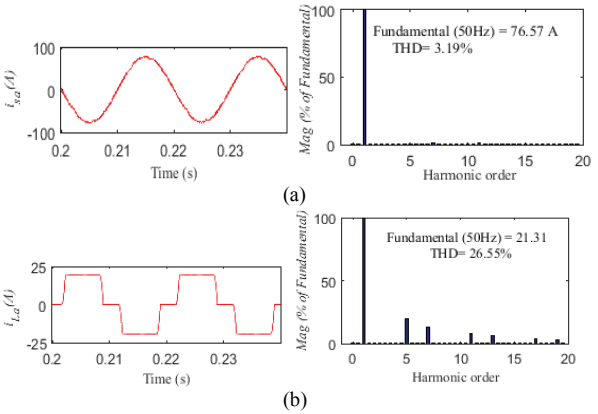

Fig 4 - Waveform and harmonic spectrum of a) grid current b) load current

B) Dynamic Behavior of Proposed Topology with Nonlinear Load

In Figs. 5 (a-b), the response of the system in unbalanced load state is observed. In this figure, V_{dc},V_{sabc}, i_{sabc}, i_{lc}, i_s*, i_{spv}, error of the adaptive component (e_{Ac}), signum function of e_{Ac} (sgn(e_{Ac})), weight of active reference component of phase c (w_{Ac}), w_{LA}, w_{pv}, w_{cA} and w_{sA} are shown. At t=0.5 s, the load of phase C is switched off, which makes the load unbalanced. The source current remains sinusoidal due to the compensating current provided by the VSC. It is observed the supply current increases in magnitude after the load is switched off. This is because only two phases of the load requires power, thus the power produced in the SPV array is directly fed to AC grid, increasing the grid current. It is observed that the weights change after the load is switched off as shown in Fig. 5 (b).

C) Behavior of Proposed Topology under Variable Insolation

In Figs. 6 (a-b), the insolation level (G), I_{pv}, V_{pv}, P_{pv}, V_{dc}, P_s, Q_s, V_{sabc}, i_{sabc}, i_{labc}, i_s*and i_{spv} are shown. The insolation level is changed from 500 to 800 W/m^2 at t = 0.8 s. The power generated in SPV array increases with higher solar insolation, increasing the SPV current as well. Thus, the power delivered to grid increases. Another observation is that the DC link voltage doesn't change much with insolation levels. It is nearly constant around the value generated by MPPT, in this case around 700V.

IV. Conclusion

The performance of proposed sign-error based adaptive control for a single stage SPV grid tied system has been studied through modeling and simulation in MATLAB in three phase distribution system. The single stage system has improved the overall efficiency. This grid integrated system has been shown to 1) provide active power to grid; 2) act as a DSTATCOM. Consequently, the THD of supply current has

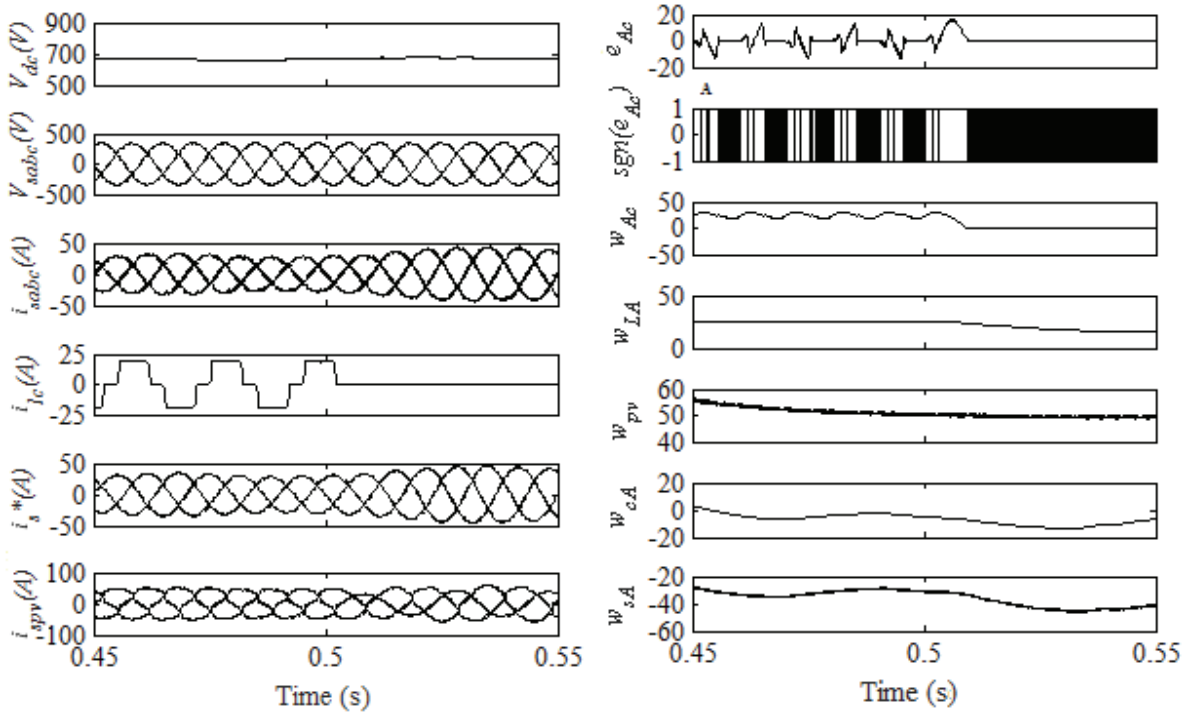

(a) (b)

Fig. 5 (a,b) - Dynamic response of the SPV grid tied system under unbalanced load condition

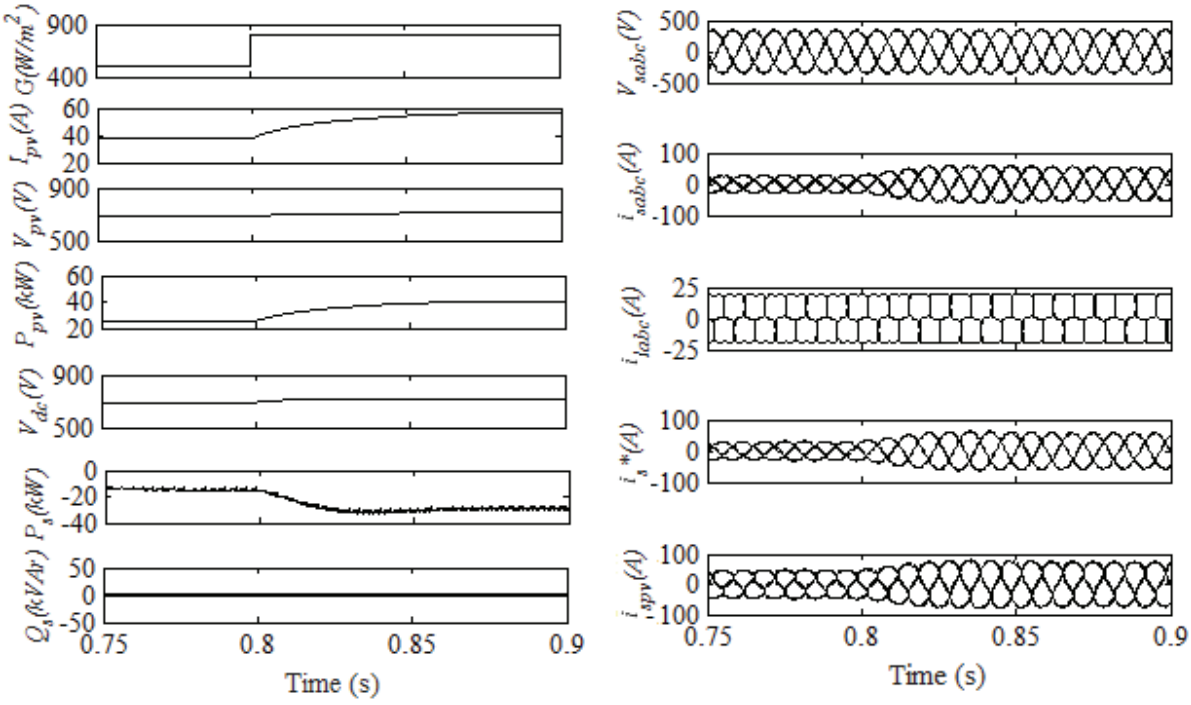

(a) (b)

Fig 6 (a, b) - Behaviour of system under variable insolation level

been reduced to acceptable levels as stated by the IEEE standard. The system has performed satisfactorily under various conditions such as variable solar insolation, unbalanced load etc.

V. ACKNOWLEDGMENT

Authors are highly thankful to DST, Govt. of India, for supporting this project under Grant Number: RP02583.

APPENDICES

SPV System Parameters: SPV module voltage, V_{MPP} = 26.3 V; SPV module current, I_{MPP} = 7.61 A; SPV array power, P_{MPP} = 50 kW; N_s = 27; N_p =9; DC bus voltage, V_{dc}= 700 V; DC bus capacitor, C_{dc}= 20 mF; interfacing inductor, L_f = 3mH; sampling time, T_s = 3μs; grid voltage, V_{LL} = 415 V (rms).

System and Load Parameters: Ripple filter, R_f = 5 Ω and C_f = 10 μF, DC PI controller, K_{pA} =1 and K_{iA} = 0.001; adaptation constant, τ_p = 0.0002; nonlinear load = 3- phase diode bridge with R = 10 Ω and L = 100 mH.

REFERENCES

[1] E. Romero-Cadaval, B. Francois, M. Malinowski, and Qing-Chang Zhong, "Grid-Connected Photovoltaic Plants: An Alternative Energy Source, Replacing Conventional Sources," *IEEE Industrial Electronics Magazine*, vol. 9, no. 1, pp. 18-32, March 2015.

[2] Bidyadhar Subudhi and R. Pradhan, "A comparative study on maximum power point tracking techniques for photovoltaic power systems," *IEEE Trans. Sus. Energy*, vol. 4, no. 1, pp. 89-98, January 2013.

[3] Tsai-Fu Wu, Chih-Hao Chang, Li-Chiun Lin and Chia-Ling Kuo, "Power loss comparison of single- and two-stage grid-connected photovoltaic systems," *IEEE Trans. on Energy Conversion*, vol. 26, no. 2, pp. 707-715, June 2011.

[4] R. Agarwal, I. Hussain and B. Singh, "LMF based control algorithm for single stage three-phase grid integrated solar PV system," *IEEE Trans. on Sustainable Energy*, Early Access, 2016.

[5] M. Singh and A. Chandra, "Real-time implementation of ANFIS control for renewable interfacing inverter in 3P4W distribution network," *IEEE Trans. Industrial Electron.*, vol. 60, no. 1, pp. 121-128, Jan. 2013.

[6] C. Jain and B. Singh, "An assessment of RAD based control algorithm for single-stage multitasking grid tied SECS," In *Proc. Innovative Applications of Computational Intelligence on Power, Energy and Controls with their impact on Humanity (CIPECH),* Ghaziabad, 2014, pp. 273-278.

[7] R. Garg, B. Singh, D. T. Shahani and C. Jain, "Dual-Tree Complex Wavelet Transform Based Control Algorithm for Power Quality Improvement in a Distribution System," *IEEE Trans. on Industrial Electronics*, *IEEE Trans. on Industrial Electronics*, Early Access, 2016.

[8] M. Srinivas, I. Hussain and B. Singh, "Combined LMS-LMF based control algorithm of DSTATCOM for power quality enhancement in distribution system," *IEEE Trans. on Industrial Electronics*, Early Access, 2016.

[9] M. Qasim, P. Kanjiya, and V. Khadkikar, "Artificial-neural-network-based phase-locking scheme for active power filters," *IEEE Trans. on Industrial Electronics*, vol.61, no.8, pp.3857-3866, Aug. 2014.

[10] P. S. R. Diniz, *Adaptive Filtering: Algorithms and Practical Implementation*, Springer Science, New York 2013.

[11] Bhim Singh, Ambrish Chandra and Kamal Al-Haddad, *Power Quality: Problems and Mitigation Techniques*, John Wiley & Sons Ltd., U.K, 2015.

[12] M. G. Villalva, J. R Gazoli and E. R. Filho, "Comprehensive approach to modeling and simulation of photovoltaic arrays," *IEEE Trans. on Power Electronics*, vol. 24, no. 5, pp. 1198-1208, May 2009.

[13] IEEE Recommended Practices and requirement for Harmonic Control on Electric Power System, IEEE Std.519, 1992.